

Isolation and Crystal Structures of Two Singlet Bis(Triarylamine) Dications with Nonquinoidal Geometries

Shijun Zheng,^{†,‡} Stephen Barlow,^{*,†,‡} Chad Risko,[†] Tiffany L. Kinnibrugh,[§] Viktor N. Khurstalev,[¶] Simon C. Jones,[†] Mikhail Yu. Antipin,^{§,¶} Neil M. Tucker,[‡] Tatiana V. Timofeeva,[§] Veaceslav Coropceanu,[†] Jean-Luc Brédas,[†] and Seth R. Marder^{†,‡}

Contribution from the School of Chemistry and Biochemistry and Center for Organic Photonics and Electronics, Georgia Institute of Technology, Atlanta, Georgia 30332-0400, USA;

Department of Chemistry, University of Arizona, Tucson, Arizona 85721, USA; Department of Natural Sciences, New Mexico Highlands University, Las Vegas, New Mexico 87701, USA;

Institute of Organoelement Compounds, Russian Academy of Sciences, Moscow, Russia

Received June 23, 2005; E-mail: stephen.barlow@chemistry.gatech.edu

Abstract: We report the first structural data for bis(diarylamine) “bipolarons”: we have isolated and crystallographically characterized salts of the dications obtained by two-electron oxidation of *E*-4,4'-[di(*p*-anisyl)amino]stilbene and *E,E*-2,5-bis{4-[di(*p*-anisyl)amino]styryl}-3,4-di(*n*-butoxy)thiophene, **[1]²⁺** and **[2]²⁺** respectively. ESR, NMR, and magnetometry suggest both species have singlet ground states. X-ray structures, together with ¹H NMR coupling constants for **[2]²⁺**, indicate geometries in which the bond lengths are shifted toward a quinoidal pattern relative to that in the neutral species, but not to a fully quinoidal extent. In particular, the bond-length alternations across the vinylenic bridging groups approach zero. DFT calculations with closed-shell singlet configurations reproduce the observed structures well. Our results indicate that singlet species for which one might expect quinoidal geometries (with differences of ca. 0.1 Å between formally single and double bonds) on the basis of a limiting valence-bond representation of the structure can, in fact, show structures with significantly different patterns of bond lengths.

Introduction

There has been considerable interest in “bipolarons” derived from two-electron oxidation of organic conjugated molecules and polymers. Bipolarons play important roles in many conducting polymers:^{1–10} the excess charge of “traditional” bipolarons, such as those found in many conducting polymers (and presumably in appropriate oligomeric model compounds^{8,11,12}), is concentrated in the middle of the bipolaron and diminishes as one moves away from this center. In other cases, particularly

small molecules with redox-active end groups,^{12–14} the excess positive charges are, at least formally, pinned at the termini of the molecule. In both types of system, the creation of bipolarons can lead to enhanced nonlinear optical properties.^{14–16}

Bis(triarylamine) derivatives can be oxidized to dications that have been described as “bipolarons” and there have been several studies of these species in solution;^{17–19} for example, the creation of highly absorbing bis(diarylamine) dications through photo-induced charge transfer between amino-stilbene dendrimers and electron acceptors has been shown to form the basis of a reverse saturable absorber system.¹⁷

Generally, molecularly based “bipolaron” species have been generated in solution and studied by electronic or vibrational spectroscopy; there is a scarcity of structural information from either NMR or crystallography, although crystal structures have been reported for a doubly oxidized oligoaniline²⁰ and for several oligothiophene dications,^{21,22} and NMR spectra have been

[†] Georgia Institute of Technology.

[‡] University of Arizona.

[§] New Mexico Highlands University.

[¶] Russian Academy of Sciences.

- Brédas, J. L.; Chance, R. R.; Silbey, R. *Phys. Rev. B* **1982**, *26*, 5843.
- Brédas, J. L.; Street, G. B. *Acc. Chem. Res.* **1985**, *18*, 309.
- Glenis, S.; Benz, M.; Legoff, E.; Schindler, J. L.; Kannewurf, C. R.; Kanatzidis, M. G. *J. Am. Chem. Soc.* **1993**, *115*, 12519.
- Krinichnyi, V. I.; Chemerisov, S. D.; Lebedev, Y. S. *Phys. Rev. B* **1997**, *55*, 16233.
- Greenham, N. C.; Shinar, J.; Partee, J.; Lane, P. A.; Amir, O.; Lu, F.; Friend, R. H. *Phys. Rev. B* **1996**, *53*, 13528.
- Krinichnyi, V. I.; Roth, H.-K.; Hinrichsen, G.; Lux, F.; Lüders, K. *Phys. Rev. B* **2002**, *65*, 155205.
- Zotti, G.; Zecchin, S.; Schiavon, G.; Vercelli, B.; Berlin, A.; Dalcanale, E.; Groenendaal, L. *Chem. Mater.* **2003**, *15*, 4642.
- Geskin, V. M.; Brédas, J.-L. *ChemPhysChem* **2003**, *4*, 498.
- Constantini, N.; Lupton, J. M. *Phys. Chem. Chem. Phys.* **2003**, *5*, 749.
- Fernandes, M. R.; Garcia, J. R.; Schultz, M. S.; Nart, F. C. *Thin Solid Films* **2005**, *474*, 279.
- Spangler, C. W.; Picchiotti, L.; Bryson, P.; Havleka, K. O.; Dalton, L. R. *J. Chem. Soc., Chem. Commun.* **1992**, 145.
- Spangler, C. W.; Bryson, P.; Liu, P.-K.; Dalton, L. R. *J. Chem. Soc., Chem. Commun.* **1992**, 253.

- Guichard, V.; Bourkba, A.; Poizat, O.; Buntinx, G. *J. Phys. Chem.* **1989**, *93*, 4429.
- Spangler, C. W.; He, M. *J. Chem. Soc., Perkin Trans. I* **1995**, 715.
- de Melo, C. P.; Silbey, R. *J. Chem. Phys.* **1988**, *88*, 2567.
- Lai, C. M.; Meng, H. F. *Phys. Rev. B* **1996**, *54*, 16365.
- Hyfield, A.; Sonnenberg, W.; Han, Y.; Spangler, L. H.; Elandalousi, E. H.; Spangler, C. W. *J. Nonlinear Opt. Phys. Mater.* **2000**, *9*, 469.
- Lambert, C.; Nöll, G. *J. Am. Chem. Soc.* **1999**, *121*, 8434.
- Low, P. J.; Paterson, M. A. J.; Goeta, A. E.; Yufit, D. S.; Howard, J. A. K.; Cherryman, J. C.; Tackley, D. R.; Brown, B. *J. Mater. Chem.* **2004**, *14*, 2516.
- Shacklette, L. W.; Wolf, J. F.; Gould, S.; Baughman, R. H. *J. Chem. Phys.* **1988**, *88*, 3955.

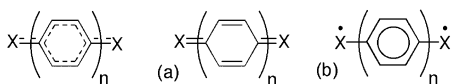
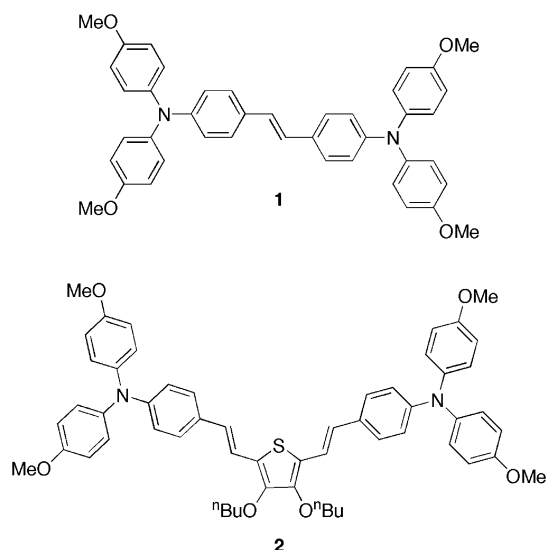


Figure 1. *p*-Phenylene-bridged species with (a) “quinoidal” and (b) biradical structures shown. X = O, NR, NR₂⁺, N₂R₃⁺, CPh₂ etc.

Chart 1



reported for a stabilized derivative of the fluorene dication.²³ In particular, bis(triarylamine) dications have not been characterized crystallographically or by NMR, although the X-ray structures of several bis(triarylamine) radical *monocations* have been recently reported.^{24–26} Here we report for the first time the isolation and crystal structures of two bis(triarylamine) dications, those of **1** and **2** (Chart 1).

For species in which two radical centers, such as $\text{—NAr}_2^{\bullet+}$, are linked by an oligo-*p*-phenylene, oligo-*p*-phenylene-vinylene, or similar conjugated bridges, i.e., for species such as $[\mathbf{1}]^{2+}$ and $[\mathbf{2}]^{2+}$, one can envisage two extreme types of structure: closed-shell singlet “quinoidal” (Figure 1a) and open-shell biradical, which may have either singlet (diamagnetic) or triplet (paramagnetic) ground states (Figure 1b). Closed-shell structures are expected if coupling through the bridge is strong, i.e., when the bridge is short and/or when its frontier orbitals are close in energy to the SOMOs of the radical end groups, X. For example, quinones (X = O) with short bridges ($n = 1, 2, 3$) are diamagnetic, while for $n = 4$ there is an equilibrium between biradical and closed-shell states;²⁷ steric effects can also lead to biradical structures, for example, in $n = 3$ quinones with bulky substituents²⁷ and in tetramethyl-*p*-phenylene bridged dihydrazine dications ($n = 1, X = \text{N}_2\text{R}_3^+$).²⁸ Closed-shell structures are often represented with four single and two double bonds within the rings and with double bonds exo to the ring,

as shown in Figure 1a. This picture is supported by crystal structures of *p*-phenylene-bridged species (Figure 1, $n = 1$) with a variety of end groups, X, including O,^{29,30} O/NOH,³¹ NR,³² and CPh₂,³³ where bond-length alternations (BLAs) of $>0.1 \text{ \AA}$ are observed between the formally double and single bonds in the ring. Indeed, this pattern of “quinoidal” BLA has been considered a signature of a closed-shell configuration; the reduced BLA found in the crystal structure of Chichibabin’s hydrocarbon (Figure 1, X = CPh₂, $n = 2$) has been interpreted as evidence for some biradical character.³³ Here we show that although $[\mathbf{1}]^{2+}$ and $[\mathbf{2}]^{2+}$ are diamagnetic, they show patterns of BLA falling well short of the ideal “quinoidal” limiting resonance forms.³⁴

Experimental Section

Synthesis. Compound **1**²⁶ and $\text{Fe}(\text{C}_5\text{H}_4\text{Ac})_2 \cdot \text{AgBF}_4^{35}$ were synthesized by literature procedures. Compound **2** was synthesized using the Horner reaction of *p*-(diarylimino)benzyl phosphonate and a thiophene dialdehyde³⁶ in a fashion similar to a closely related compound described in ref 37 (see Supporting Information for details). Other materials were obtained from commercial sources and used without further purification. In addition to synthesizing the dications as isolable salts (described below), we also generated the dications of **1** and **2** in CH_2Cl_2 solution for optical spectroscopic characterization using in situ oxidation with two equivalents of $[(p\text{-BrC}_6\text{H}_4)_3\text{N}]^+[\text{SbCl}_6]^-$ ($E_{1/2} = +0.70 \text{ V vs FeCp}_2^{+/0}$).³⁸

$[\mathbf{1}]^{2+}([\text{SbCl}_6]^-)_2$. Antimony pentachloride (0.9 mL of a 1.0 M solution in dichloromethane, 0.9 mmol) was added by syringe to a solution of **1** (175 mg, 0.258 mmol) in dry dichloromethane (3 mL). The solution instantly darkened and some precipitation occurred. After 5 min, dry diethyl ether (20 mL) was added to complete precipitation of the product; the supernatant was removed by filter cannula and the resulting powder was washed with dry diethyl ether ($2 \times 20 \text{ mL}$) and dried under reduced pressure. The product was crystallized by layering a filtered solution in dichloromethane (20 mL) with diethyl ether (100 mL); when the solvents had mixed fully, the supernatant was removed by cannula and the black microcrystalline material was washed with ether ($3 \times 10 \text{ mL}$) and dried under reduced pressure (266 mg, 0.204 mmol, 79%). Single crystals were obtained by a second dichloromethane/diethyl ether layering. Anal. Calcd. for $\text{C}_{42}\text{H}_{38}\text{Cl}_{12}\text{N}_2\text{O}_4\text{Sb}_2$: C, 38.69; H, 2.94; N, 2.15.

- (21) Kozaki, M.; Tonezawa, Y.; Okada, K. *Org. Lett.* **2002**, *4*, 4535.
 (22) Nishinaga, T.; Wakamiya, A.; Yamazaki, D.; Komatsu, K. *J. Am. Chem. Soc.* **2004**, *126*, 3163.
 (23) Nishinaga, T.; Inoue, R.; Matsuura, A.; Komatsu, K. *Org. Lett.* **2002**, *4*, 4117.
 (24) Low, P. J.; Paterson, M. A. J.; Puschmann, H.; Goeta, A. E.; Howard, J. A. K.; Lambert, C.; Cherryman, J. C.; Tackley, D. R.; Leeming, S.; Brown, B. *Chem. Eur. J.* **2004**, *10*, 83.
 (25) Szeghalmi, A. V. et al. *J. Am. Chem. Soc.* **2004**, *126*, 7834.
 (26) Barlow, S. et al. *Chem. Commun.* **2005**, 764.
 (27) Rebmann, A.; Zhou, J.; Schuler, P.; Rieker, A.; Stegmann, H. B. *J. Chem. Soc., Perkin Trans. 2* **1997**, 1615.
 (28) Nelsen, S. F.; Ismagilov, R. F.; Teki, Y. *J. Am. Chem. Soc.* **1998**, *120*, 2200.

- (29) Staab, H. A.; Jörens, M.; Krieger, C.; Rentzea, M. *Chem. Ber.* **1985**, *118*, 796.
 (30) Irngartinger, H.; Herpich, R. *Eur. J. Org. Chem.* **1998**, 595.
 (31) Sardone, N.; Carugo, O.; Charalambous, J.; Raghvani, D. V. *Acta Crystallogr.* **1996**, *C52*, 3202.
 (32) Sifi, O.; Braunstein, P. *Chem. Commun.* **2000**, 2223.
 (33) Montgomery, L. K.; Huffman, J. C.; Jurczak, E. A.; Grendze, M. A. *J. Am. Chem. Soc.* **1986**, *108*, 6004.
 (34) During the review process for our paper, another paper has appeared describing a molecule with some similarities to our dications, the neutral “extended viologen” obtained by two-electron reduction of 4,4’-bis(1-*n*-octylpyridinium-4-yl)biphenyl (Porter, W. M.; Vaid, T. P.; Rheingold, A. L. *J. Am. Chem. Soc.* **2005**, *127*, 16559). In contrast to our dications, there is significant population of the triplet in solution at room temperature; however, the authors consider this less likely in the crystal and, as with our dications, both the crystal structure and DFT results for a closed-shell singlet configuration show quinoidal BLAs of ca. 0.06 Å in the bridging phenylene groups. The phenylene-phenylene and phenylene-pyridinium bonds are also considerably longer than typical double bonds according to both X-ray and DFT data.
 (35) Carty, P.; Dove, M. F. A. *J. Organomet. Chem.* **1971**, *28*, 125.
 (36) Ono, N.; Okumura, H.; Murashima, T. *Heteroatom Chem.* **2001**, *12*, 414.
 (37) Zheng, S. J.; Barlow, S.; Parker, T. C.; Marder, S. R. *Tetrahedron Lett.* **2003**, *44*, 7989.
 (38) Connelly, N. G.; Geiger, W. E. *Chem. Rev.* **1996**, *96*, 877.

Found: C, 39.09; H, 2.96; N, 2.19. UV–vis–NIR (CH₂Cl₂, generated in situ) λ_{\max} (ϵ_{\max}) 900 (129 000) nm (M⁻¹cm⁻¹). IR (KBr) ν 1602 (s), 1587 (s, br), 1498, 1460, 1438, 1307, 1262 (s, br), 1191 (w), 1158 (s), 1116, 1020, 925 (w), 834, 804, 647, 578, 524 (w), 505 (w) cm⁻¹.

[2]²⁺[(SbF₆)⁻]₂. To a solution of compound **2** (84 mg, 0.095 mmol) in dichloromethane (5 mL) was added AgSbF₆ (65 mg, 0.19 mmol) at room temperature under nitrogen atmosphere. The resulting solution was stirred for 5 min, then filtered into a vial and layered with pentane under nitrogen atmosphere. After 2 days, filtration gave dark brown crystals (100 mg, 78%). ¹H NMR (CD₂Cl₂, 400 MHz, -85 °C, with Fe(C₅H₄Ac)₂·AgBF₄ added to remove traces of the monocation) δ 7.95 (d, *J* = 8.8 Hz, 2H), 7.76 (d, *J* = 13.5 Hz, 2H), 7.58 (m, 4H), 7.18 (bs, 8H), 7.11 (d, *J* = 8.7 Hz, 2H), 7.07 (d, *J* = 8.5 Hz, 2H), 6.98 (m, 8H), 4.21 (bs, 4H), 3.82 (s, 12H), 1.72 (bs, 4H), 1.41 (bs, 4H), 0.77 (bt, *J* = 7.6 Hz, 6H). HRMS (FAB⁺) calcd for C₅₆H₅₈N₂O₆S (M⁺-2SbF₆): 886.4005; Found: 866.3992. Anal. Calcd for C₅₆H₅₈F₁₂N₂O₆SSb₂: C, 49.51; H, 4.30; N, 2.06. Found: C, 49.66; H, 4.33; N, 1.97. UV–vis–NIR (CH₂Cl₂, generated in situ) λ_{\max} (ϵ_{\max}) 1072 (85 900) nm (M⁻¹cm⁻¹).

X-ray Crystal Structures. All data were acquired at 120(2) K using Mo–K α radiation (λ = 0.71073 Å). Structures were refined using full-matrix least squares against *F*². Parameters relating to the crystal structure data collection and refinements are tabulated in the Supporting Information; CIF files are also included in the Supporting Information. The experimental data indicated positional static disorder in some of the terminal groups of [1]²⁺[(SbCl₆)⁻]₂ and [2]²⁺[(SbF₆)⁻]₂. To model the disorder in cation [1]²⁺, two possible sets of atomic positions were included in the refinement for one of the anisyl fragments (C16–C21, O2); populations of the two positions were obtained in ratio 0.7:0.3. In cation [2]²⁺ two possible positions were considered for carbon atoms in two of the methoxy groups (C26 and C49) and for one of the *n*-butyl groups (C27–C30). The ratios of occupancies after refinement were 0.55:0.45 (atoms C34/C34'), 0.65:0.53 (atoms C48/C48') and 0.50:0.50 (atoms C53–C56/C53'–C56', isotropic refinement only). In the figures the positions of less populated sites in the disordered fragments are omitted for clarity.

Computational Details. Geometries for the neutral, radical-cation, and dication states of **1** and **2**, and for the neutral Chichibabin hydrocarbon were obtained using Density Functional Theory (DFT). In the cases of [1]²⁺, [2]²⁺, and Chichibabin's hydrocarbon, closed-shell singlet, biradical (broken symmetry), and triplet configurations were taken into consideration. The DFT calculations were carried-out using the B3LYP functional, where Becke's three-parameter hybrid exchange functional is combined with the Lee–Yang–Parr correlation functional,^{39–41} with a 6-31G* split valence plus polarization basis set. All DFT calculations were performed with Gaussian98 (Rev. A.11).⁴²

Results and Discussion

Synthesis. Compound **1** was synthesized using the palladium-catalyzed C–N coupling^{43,44} of *E*-4,4'-dibromostilbene⁴⁵ with

- (39) Becke, A. D. *Phys. Rev.* **1988**, *A38*, 3098.
 (40) Becke, A. D. *J. Chem. Phys.* **1993**, *98*, 5648.
 (41) Lee, C. T.; Yang, W. T.; Parr, R. G. *Phys. Rev.* **1988**, *B37*, 785.
 (42) Frisch, M. J. et al. *Gaussian98, Rev. A.11*, 1998.
 (43) Driver, M. S.; Hartwig, J. F. *J. Am. Chem. Soc.* **1996**, *118*, 7217.

Table 1. Electrochemical Potentials (V vs [FeCp₂]⁺⁰), with Relative Peak Heights in Parentheses, for Compounds **1** and **2** in CH₂Cl₂ / 0.1 M [¹⁸Bu₄N]⁺[PF₆]⁻

	<i>E</i> _{1/2} ⁺⁰	<i>E</i> _{1/2} ^{2+/+}	<i>E</i> _{1/2} ^{3+/2+}	<i>E</i> _{1/2} ^{4+/3+}
1	+0.08(1)	+0.22(1)	-	-
2		+0.05(2) ^a	+0.70(1)	+1.05(1)

^a Two overlapping one-electron processes.

di-p-anisylamine;^{46,47} full details are provided in the Supporting Information of ref 26. Compound **2** was synthesized using the Horner reaction^{48,49} of a diformylthiophene³⁶ with the *p*-(diarylamino)benzyl phosphonate, which was itself prepared using a general method we have recently described;³⁷ full details are provided in the Supporting Information. Electrochemical data (see Supporting Information for details) for **1** and **2** are summarized in Table 1; both compounds may be oxidized readily and reversibly to the corresponding dications; the potentials are close to those for other bis(*di-p*-anisylamino) systems suggesting these oxidations are principally triarylamino-centered,^{18,50–52} consistent with calculations of charge distribution (*vide infra*) and with the ESR spectrum of [1]²⁺.²⁶ In the case of **2**, oxidations to tri- and tetracationic species are also observed and are presumably associated with the bridging dialkoxythiophene unit. Analytically pure crystalline [1]²⁺[(SbCl₆)⁻]₂ was isolated after oxidation of neutral **1** with ca. three equivalents of SbCl₅ in dichloromethane, followed by precipitation with diethyl ether and by recrystallization by layering a dichloromethane solution with diethyl ether. Analytically pure [2]²⁺[(SbF₆)⁻]₂ was isolated after oxidation of neutral **2** with two equivalents of AgSbF₆ in dichloromethane, followed by filtration and layering with pentane.

NMR. Both dications were found to have diamagnetic ground states. We found a solid sample of [2]²⁺[(SbF₆)⁻]₂ to be weakly paramagnetic; SQUID magnetometry shows Curie behavior corresponding to $\mu_{\text{eff}} \approx 0.02 \mu_{\text{B}}$, indicating this paramagnetism is likely to be due to an impurity, presumably the corresponding monocation. NMR studies of the dication are, therefore, potentially complicated by electron exchange with traces of the monocation; moreover, we also encountered complications due to restricted rotation. However, we were able to obtain reasonably well-resolved ¹H NMR spectra of [2]²⁺ at -85 °C (where the restricted rotation is in the slow régime) in the presence of a small amount of Fe(C₅H₄Ac)₂·AgBF₄³⁵ (we found this oxidizing agent removed monocation impurities while not over-oxidizing to create [2]³⁺) and to assign it using ¹H-¹H COSY and NOESY experiments: the COSY spectrum is shown in Figure 2; additional NMR spectra of [2]²⁺ are given in the Supporting Information. In the case of [1]²⁺ we were unable to acquire useful NMR spectra due to paramagnetism. However, Evans' method NMR⁵³ (room temperature, CD₂Cl₂, 400 MHz;

- (44) Wolfe, J. P.; Wagaw, S.; Buchwald, S. L. *J. Am. Chem. Soc.* **1996**, *118*, 7215.
 (45) Baumgarten, M.; Yuksel, T. *Phys. Chem. Chem. Phys.* **1999**, *1*, 1699.
 (46) Zhao, H.; Tanjutco, C.; Thayumanavan, S. *Tetrahedron Lett.* **2001**, *42*, 4421.
 (47) Kauffman, J. M.; Moyna, G. *J. Org. Chem.* **2003**, *68*, 839.
 (48) Horner, L. *Chem. Ber.* **1958**, *83*, 733.
 (49) Wadsworth, W. S.; Emmons, W. D. *J. Am. Chem. Soc.* **1961**, *83*, 1733.
 (50) Seo, E. T.; Nelson, R. F.; Fritsch, J. M.; Marcoux, L. S.; Leedy, D. W.; Adams, R. N. *J. Am. Chem. Soc.* **1966**, *88*, 3498.
 (51) Jones, S. C.; Coropceanu, V.; Barlow, S.; Kinnibrugh, T.; Timofeeva, T.; Brédas, J.-L.; Marder, S. R. *J. Am. Chem. Soc.* **2004**, *126*, 11782.
 (52) Lambert, C.; Risko, C.; Coropceanu, V.; Schelter, J.; Amthor, S.; Gruhn, N. E.; Durivage, J. C.; Brédas, J. L. *J. Am. Chem. Soc.* **2005**, *127*, 8508.
 (53) Grant, D. H. *J. Chem. Ed.* **1995**, *72*, 39.

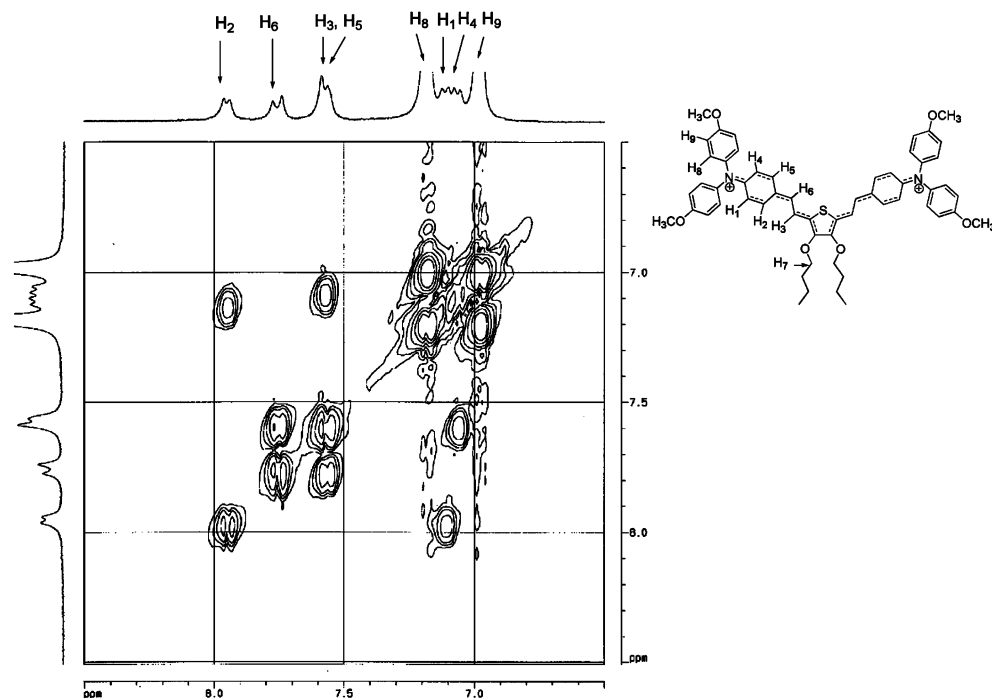


Figure 2. ^1H - ^1H COSY NMR spectrum of the aromatic and vinylic region of $[2]^{2+}([\text{SbF}_6]^-)_2$ at $-85\text{ }^\circ\text{C}$ in CD_2Cl_2 .

no measurable contact shift, indicating $\mu_{\text{eff}} < 0.3\ \mu_{\text{B}}$, ESR (CH_2Cl_2 , room temperature, weak signal with integration corresponding to ca. 6% $S = 1/2$ molecules⁵⁴), and SQUID magnetometry (solid state, Curie behavior, $\mu_{\text{eff}} < 0.1\ \mu_{\text{B}}$) together support an impurity origin for this paramagnetism. These data are, therefore, all consistent with singlet ground states for both species with negligible population of any high-spin states at room temperature.

^1H NMR spectra of $[2]^{2+}$ at $-85\text{ }^\circ\text{C}$ indicate that rotation around the $\text{C}_6\text{H}_4\text{-CH}$ bond is slow (as indicated by the inequivalence of H1 and H4 and of H2 and H5, as seen in Figure 2, and by the observation of a NOE between H3 and H7, but not between H6 and H7), indicating some multiple bond character. However, the coupling constant between the two vinylic protons (H3 and H6) is ca. 13.5 Hz, falling in the range found for symmetric polymethines (bond order = 1.5),^{55,56} rather than the ca. 10 Hz or ca. 16 Hz expected for trans-CH=CH- and =CH-CH= entities, respectively.⁵⁷ Thus NMR indicates that $[2]^{2+}$ has neither a benzenoid structure similar to that of the neutral species nor the structure suggested by a limiting quinoidal resonance structure, but lies between these extremes.

Crystal Structures and Calculated Geometries. We determined the structures of $[1]^{2+}([\text{SbCl}_6]^-)_2$ (Figure 3), **2**, and $[2]^{2+}([\text{SbF}_6]^-)_2$ (Figure 4) by X-ray crystallography; some parameters are compared in Table 2 with analogous values from

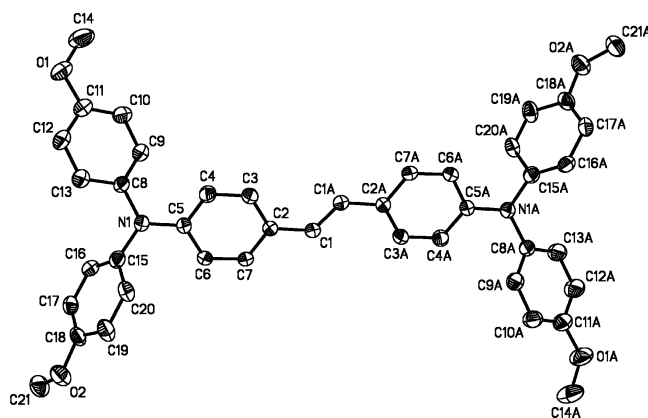


Figure 3. View of $[1]^{2+}$ in the crystal structure of its $[\text{SbCl}_6]^-$ salt. Atoms "A" are generated by C_i symmetry. Thermal ellipsoids are at 50% probability and all H atoms have been omitted.

the previously reported structures of **1** and $[1]^+[\text{SbF}_6]^-$.²⁶ The $[1]^{n+}$ system is a rare example of a dinuclear mixed-valence system where all three oxidation states are structurally characterized; the only previous example of which we are aware has dimolybdenum redox centers and, as in the $[1]^{n+}$ system, the monocation is a Robin-Day class-III⁵⁸ mixed-valence compound and the dication is a singlet.⁵⁹ The data for the $[1]^{n+}$ system show that successive oxidation of **1** results in increased shortening of the $\text{N-C}_6\text{H}_4$ bond and increased BLA with a quinoidal sense in the bridging phenylene groups. Interestingly, however, the BLA in the dication falls well short of the "ideal" quinoidal BLA of ca. $0.1\ \text{\AA}$ that we originally expected based on the alternating single and double bonds of the limiting resonance structure.³⁴ The vinylene bridge of $[1]^{2+}$ retains the same sense of BLA as the neutral species, although with a greatly reduced magnitude. The experimental geometry of $[1]^{2+}$

(54) We observed a three-line spectrum ($g = 2.004$; $A_{\text{N}} = \text{ca. } 9\ \text{G}$) characteristic of a localized triarylammonium cation (Seo, E. T.; Nelson, R. F.; Fritsch, J. M.; Marcoux, L. S.; Leedy, D. W.; Adams, R. N. *J. Am. Chem. Soc.* **1966**, *88*, 3498; Bamberger, S.; Hellwinkel, D.; Neugebauer, F. A. *Chem. Ber.* **1975**, *108*, 2416), unlike the five-line spectrum we see for $[1]^+$ or the featureless spectra we see for other bis(diarylamino) phenylene-vinylene dications (Barlow, S.; Risko, C.; Chung, S.-J.; Tucker, N. M.; Coropceanu, V.; Jones, S. C.; Levi, Z.; Brédas, J. L.; Marder, S. R. *J. Am. Chem. Soc.* **2005**, *127*, 16900).

(55) Tolbert, L. M.; Zhao, X. *J. Am. Chem. Soc.* **1997**, *119*, 3253.

(56) Barlow, S.; Henling, L. M.; Day, M. W.; Schaefer, W. P.; Green, J. C.; Hascall, T.; Marder, S. R. *J. Am. Chem. Soc.* **2002**, *124*, 6285.

(57) Pretsch, E.; Bühlmann, P.; Affolter, C. *Structure Determination of Organic Compounds*; Springer-Verlag: Berlin, 2000.

(58) Robin, M. B.; Day, P. *Adv. Inorg. Chem. Radiochem.* **1967**, *10*, 247.

(59) Cotton, F. A.; Liu, C. Y.; Murillo, C. A.; Villagrán, D.; Wang, X. *J. Am. Chem. Soc.* **2004**, *126*, 14882.

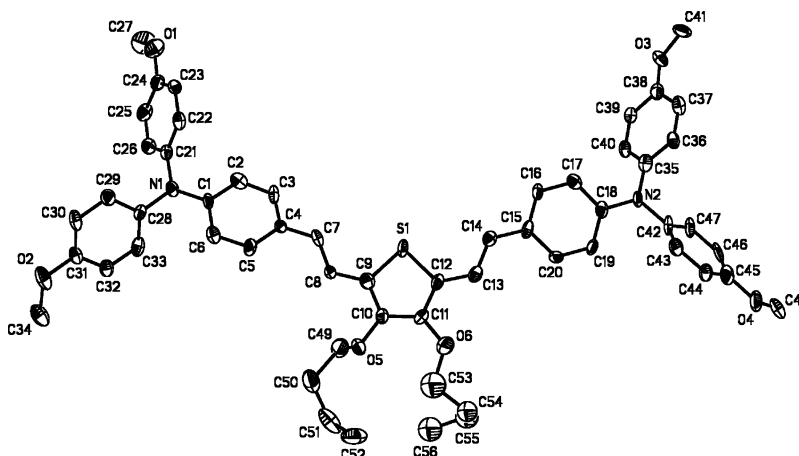


Figure 4. View of $[2]^{2+}$ in the crystal structure of its $[SbF_6]^-$ salt showing only one of the possible orientations for the disordered C34, C48, C55 and C56 atoms. Thermal ellipsoids are at 50% probability and all H atoms have been omitted.

Table 2. Selected Bond Lengths (Å) for **1** and **2** and Their Monocations and Dications from X-ray and DFT^a(in italics)

	An–N	N–C ₆ H ₄	BLA(C ₆ H ₄) ^b	C ₆ H ₄ –CH	CH=CH ^c	CH–C _{thi} ^c	(C=C) _{thi} ^c	(C–C) _{mi} ^c
1 ^d	1.435(3) <i>1.425</i>	1.389(2) <i>1.413</i>	0.021(3) <i>0.021</i>	1.447(3) <i>1.461</i>	1.343(4) <i>1.352</i>	-	-	-
[1] ^{+d}	1.431(3) <i>1.429</i>	1.369(8) <i>1.388</i>	0.034(14) <i>0.042</i>	1.473(16) <i>1.436</i>	1.316(6) <i>1.370</i>	-	-	-
[1] ²⁺	1.424(2) <i>1.423</i>	1.369(5) <i>1.379</i>	0.058(3) <i>0.056</i>	1.417(5) <i>1.420</i>	1.370(7) <i>1.385</i>	-	-	-
<i>Singlet</i>	<i>1.423</i>	<i>1.379</i>	<i>0.056</i>	<i>1.420</i>	<i>1.385</i>	-	-	-
<i>BS</i>	<i>1.414</i>	<i>1.407</i>	<i>0.033</i>	<i>1.450</i>	<i>1.362</i>	-	-	-
<i>Triplet</i>	<i>1.410</i>	<i>1.419</i>	<i>0.024</i>	<i>1.460</i>	<i>1.354</i>	-	-	-
2	1.423(4) <i>1.425</i>	1.409(4) <i>1.412</i>	0.010(3) <i>0.022</i>	1.456(3) <i>1.457</i>	1.327(6) <i>1.356</i>	1.440(3) <i>1.438</i>	1.368(2) <i>1.385</i>	1.417(3) <i>1.427</i>
[2] ²⁺	1.430(7) <i>1.430</i>	1.384(2) <i>1.373</i>	0.023(8) <i>0.058</i>	1.404(2) <i>1.414</i>	1.387 <i>1.391</i>	1.376(4) <i>1.397</i>	1.406(4) <i>1.423</i>	1.382(11) <i>1.397</i>
<i>Singlet</i>	<i>1.430</i>	<i>1.373</i>	<i>0.058</i>	<i>1.414</i>	<i>1.391</i>	<i>1.397</i>	<i>1.423</i>	<i>1.397</i>
<i>BS</i>	<i>1.422</i>	<i>1.391</i>	<i>0.044</i>	<i>1.432</i>	<i>1.375</i>	<i>1.414</i>	<i>1.408</i>	<i>1.412</i>
<i>Triplet</i>	<i>1.417</i>	<i>1.405</i>	<i>0.035</i>	<i>1.445</i>	<i>1.365</i>	<i>1.426</i>	<i>1.398</i>	<i>1.423</i>

^a DFT values for dications are for the closed-shell singlet, broken-symmetry “biradical singlet” (BS), and biradical triplet configurations. ^b Difference between average C_{ipso}–C_o and C_m–C_p and average C_o–C_m bond lengths; i.e., bonds expected to be long and short respectively in a quinoidal structure. ^c Double or single bonds indicate the formal order of bonds in the neutral structures shown in Chart 1; “_{thi}” denotes the thiophene unit of $[2]^{n+}$. ^d Ref 26.

is consistent with that obtained from B3LYP/6-31G* DFT calculations (also in Table 2) for a closed-shell singlet configuration; calculations for a triplet configuration show a rather different geometry characterized by more-or-less equal shortening of all C–N bonds on oxidation and by retention of stronger BLA in the vinylene bridge, while the results obtained by a broken-symmetry (BS) DFT method⁶⁰ suggest that the geometry of the open-shell singlet (“singlet biradical”) configuration is intermediate between that of the closed-shell singlet and the triplet biradical. Thus, comparison of the X-ray data and DFT results strongly support a closed-shell singlet configuration for $[1]^{2+}$.⁶¹ Moreover, the X-ray and DFT results both indicate that closed-shell singlet structures such as $[1]^{2+}$, for which one might expect a canonical “quinoidal” pattern of BLA, can, in fact, show significant deviation from this pattern.³⁴

Our crystals of $[2]^{2+}$ were of poorer quality than those of $[1]^{2+}$, and refinement was more complicated by disorder; consequently some of the geometric parameters are somewhat less precisely determined than those of $[1]^{2+}$ and, in particular, the BLA pattern in the phenylene groups is less well-defined.

However, the pattern suggested by both crystallography and DFT is similar to that for $[1]^{2+}$; i.e., oxidation shifts the bond length pattern in the quinoidal direction so that the bonds across the vinylene groups are all approximately equal, consistent with the ¹H NMR data. A similar pattern of less than “fully quinoidal” geometry is found within the thiophene ring; previous crystal structures of “fully quinoidal” thiophene derivatives^{62–64} reveal differences of ca. 0.06 Å between long and short bonds, i.e., greater than that seen or calculated here.

It is worth emphasizing again that BLAs of ca. 0.1 Å have been taken as characteristic of closed-shell structures,³³ yet here we find considerably reduced BLA in both dications.³⁴ Moreover, we have also revisited the geometry of Chichibabin’s hydrocarbon (Figure 1, *n* = 2, X = CPh₂), for various electronic configurations (see Supporting Information); this species is isoelectronic with 4,4’-bis(diarylamino)biphenyl dications. The electronic structure of this compound has been controversial, in part because its poor solubility has hampered purification and led to complications in spectroscopic investigations; however, an X-ray structure showing less than quinoidal BLA has been taken as evidence of biradical character.³³ While in

(60) The broken-symmetry unrestricted DFT method does not produce a well-defined spin state, but rather a mixture of singlet and triplet states. Open-shell singlet states generally require a multi-configurational self-consistent-field treatment.

(61) The DFT method does not allow us to treat possible configuration interaction between closed- and open-shell singlet configurations; however, comparison of the X-ray geometry and the DFT results strongly suggest that the closed-shell configuration is dominant.

(62) Pappenfus, T. M.; Raff, J. D.; Hukkanen, E. J.; Burney, J. R.; Casado, J.; Drew, S. M.; Miller, L. L.; Mann, K. R. *J. Org. Chem.* **2002**, *67*, 6015.

(63) Murakami, F.; Sasaki, S.; Yoshifuji, M. *Angew. Chem., Int. Ed. Engl.* **2002**, *41*, 2574.

(64) Casado, J.; Pappenfus, T. M.; Mann, K. R.; Ortí, E.; Viruela, P. M.; Milián, B.; Hernández, V.; Navarreye, J. T. L. *ChemPhysChem* **2004**, *5*, 529.

this case the geometry of the broken-symmetry state is closest to the experimental X-ray geometry,³³ it is interesting that the calculated closed-shell singlet geometry is characterized by a less than fully quinoidal BLA (0.076 Å) and a rather long C₆H₄–C₆H₄ bond (1.420 Å).

Charge Distribution. Finally we return to the issue of the distribution of the excess charge in “bipolarons”. As a simple indicator of the charge distributions in the positively charged species, we have calculated the change in Mulliken charges, Δq , associated with oxidation from neutral to monocations and closed-shell singlet dications for **1** and **2**, and also for one-electron oxidation of the model compound *N,N*-di-*p*-anisylaniline. The patterns of Δq are very similar for both mono- and dications, with the magnitude of Δq for each atom in the dication approximately twice that of the corresponding atom in the monocation, consistent with the observation that the monocation geometries are intermediate between the neutral and dication geometries. The Δq on nitrogen atoms of the dications (+0.065 and +0.051 electronic charges for [**1**]²⁺ and [**2**]²⁺ respectively) is only a little smaller than that for the *N,N*-di-*p*-anisylaniline cation (+0.076), and there is a similar pattern of Δq in the terminal *p*-anisyl groups; these findings suggest that the oxidations are principally triarylamine-based, broadly consistent with the charge distribution implied by simple resonance structures. However, significant Δq are found throughout the π -systems of both molecules ($\Delta q = +0.054$ per vinylene carbon of [**1**]²⁺; average Δq per vinylene atom of [**2**]²⁺ = +0.034; average Δq per dialkoxythiophene S, O and sp²-C atom of [**2**]²⁺ = +0.032), thus indicating the true charge distribution in these species is less clear-cut than that implied by quinoidal resonance structures. This finding is consistent with the type of charge distributions proposed for the “polaron lattice” configuration of conducting polyaniline (emeraldine salt).^{65,66}

Summary

We have reported the first crystal structures of bis(triarylamine) dications, both of which are ground-state singlets.

Crystallographic (and, for [**2**]²⁺, NMR) data indicate oxidation results in a shift in the bond lengths toward a quinoidal structure, but not to the “fully quinoidal” extent one might expect based upon the limiting valence-bond representations of the structures. DFT calculations for closed-shell singlet configurations give similar structures, suggesting that significant open-shell character need not be invoked to explain these geometries. Thus, we have shown that in molecules of the type generalized in Figure 3 one cannot necessarily anticipate the same patterns of quinoidal BLA that are seen in “typical” quinones, even for species with closed-shell singlet configurations; the bond-length and charge-distribution patterns described here are in fact reminiscent of those proposed for the “polaron lattice” configuration of conducting polyaniline.

Acknowledgment. This material is based upon work supported in part by the STC Program of the National Science Foundation under Agreement Number DMR-0120967. We also thank the NSF for funding through grant CHE-0342321, the Defense Advanced Research Projects Agency for funding through the MORPH program, and the National Institute of Health for funding through the RIMI program (award number 1P20MD001104-01). We thank Man Han and Prof Z. John Zhang for assistance with SQUID measurements.

Supporting Information Available: Complete ref 25, 26 and 41; details of physical measurements and synthesis of **2**; ¹H and NOESY NMR spectra for [**2**]²⁺; additional crystallographic experimental details including figure showing X-ray structure of **2**; tables of calculated geometries for **1**, [**1**]⁺, [**1**]²⁺, **2**, [**2**]⁺, [**2**]²⁺ and the Chichibabin hydrocarbon; and full xyz coordinates for calculated structures (pdf format). X-ray data (CIF format). This material is available free of charge via the Internet at <http://pubs.acs.org>. See any current masthead page for ordering information and Web access instructions.

(65) Stafström, S.; Brédas, J. L.; Epstein, A. J.; Woo, H. S.; Tanner, D. B.; Huang, W. S.; MacDiarmid, A. G. *Phys. Rev. Lett.* **1987**, *59*, 1464.

(66) Libert, J.; Brédas, J. L.; Epstein, A. J. *Phys. Rev. B* **1995**, *51*, 5711.